Journal of Optoelectronics and Advanced Materials Vol. 2, No. 5, 2000, p. 498-514

Section 2: Organic materials *INVITED*

ELECTRICAL AND PHOTOELECTRICAL PROPERTIES OF THE SINGLE-, AND MULTI - LAYER ORGANIC PHOTOVOLTAIC CELLS

S. Antohe

Faculty of Physics, University of Bucharest, P.O.Box MG-11, Bucharest-Magurele, 76900 ROMANIA

In this work are summarized the electrical and photoelectrical properties of the organic photovoltaic cells based on the organic thin layers. Starting with the single-layer photovoltaic structures, the ITO/CuPc/Al and ITO/TPyP/Al has been prepared and characterized, where the organic layers of CuPc and TPyP, are Copper Phthalocyanine and 5,10,15,20-Tetra (4-Pyrydil)21H,23H-Porphine, respectively. The photovoltaic structures based on the p-n heterojunction present at the interface between two organic layers, like, ITO/CuPc/TPyP/Al and ITO/Chl a/TPyP/Al, exhibits stronger spectral sensitivity and better spectral matching to a solar spectrum than Schottky cells using either CuPc or TPyP, layer. Three-layered organic solar cells with an interlayer of codeposited dyes of p-type CuPc and n-type TPyP, between the respective dye layers were also prepared and characterized. They showed increased power conversion efficiency, due to the efficient carrier photogeneration in enlarged photoactive region from the codeposited layer.

Keywords: Photovoltaics, Organic semiconductors, Phthalocyanines

1. Introduction

In the latest years, there has been considerable interest in the study of organic monomeric and polymeric materials, which make them attractive candidates for use in electronic and optoelectronic devices. There has been a great deal of interest in the photovoltaic properties of the organic semiconductors because of their potential use as inexpensive material for solar cells and because of their high optical absorption in visible region of the solar spectrum. Among the organic materials, which have been studied from this point of view, were the merocyanines [1-2], phthalocyanines [3-6] and porphyrins [7-9]. The scored progresses in the understanding of photovoltaic mechanism and the development of organic solar cells technologies determined the increase of power conversion efficiency by 10^{-5} % in 1970 to 2% in our days, see Table 1.

Table 1. The parameters obtained for the organic solar cells.

Data	Cell structure	η_e (%)	U_{oc} (V)	FF	Reference
1974	Al/MgPc/Ag	0.001	0.85	0.25	[17]
1975	Cr/Clorofila-a/Hg	0.001	0.32	0.25	[18]
1977	Al/TPP/Ag	0.01	0.60	-	[7]
1978	In/ZnPc/Au	0.01	0.22	0.48	[19]
1980	Al/merocianina+I_2/Au	0.31	0.70	0.35	[20]
1981	Al/merocianina+Cl_2/Au	0.36	0.74	0.39	[21]
1983	NESA/CdS/MgPc/Al	0.128	0.45	0.29	[22]
1984	Au/ZnPc/TPyP/Al	2.00	1.00	0.25	[10]
1986	ITO/CuPc/PV/Ag	1.00	0.45	0.65	[11]
1989	ITO/CuPc/Al	0.006	0.68	0.35	[23]
1991	ITO/CuPc/TPyP/Al ITO/MePTC/MePTC+H_2Pc/H_2Pc/Au	0.12 0.70	0.40 0.50	0.44 0.45	[5] [12]
1992	ITO/CdS/CuPc/Cu	0.115	0.38	0.53	[6]
1993	ITO/TPyP/Al	0.027	0.17	0.13	[9]
1996	ITO/Chl-a/TPyP/Al ITO/CuPc/(CuPc+TPyP)/TPyP/Al	0.011 0.35	0.49 0.405	0.34 0.32	[24] [25]
2000	ITO/a-Si:H p-i-n/TPyP/Au	3.22	0.346	0.58	[28]

Most of the organic cells have been of Schottky type, in which an organic layer is sandwiched between two electrodes having suitable work function, one of them forming a rectifying contact and the other one forming an ohmic contact with the dye layer [1-3, 7-9]. There are some factors, which limit the performances of an organic Schottky cell, having generally low power conversion efficiency, smaller than 1%. A higher power conversion efficiency, of about 0.1-2%, has been achieved from the two-layer organic photovoltaic cells [2, 5-6, 10-11]. In these devices, the interface between the two organic materials, rather than electrode/organic contacts, is crucial in determining the photovoltaic response. The absorption characteristics of the two layers, if complementary, enhance substantially the utilization of wavelengths of solar spectrum by the two-layer cell as compared with single-layer cell.

Recently, internal power conversion efficiency of 0.7% was obtained [12], from a three-layered organic solar cell with photoactive interlayer of codeposited pigments, which has been found to act as an efficient carrier photogeneration layer. Afterwards, we have reported the strong "cosensitization" effect [5], presented by the two-layer organic photovoltaic cell fabricated from Copper Phthalocyanine (CuPc) as p-type organic semiconductor and 5,10,15,20-tetra-(4-pyridil)21H,23H-porphine (TPyP) as n-type organic semiconductor. Motivated by the encouraging results on heterojunction CuPc/TPyP devices and in an effort to obtain a thicker photoactive region at the interface between the two-organic layers, we have fabricated the three-layered organic cells ITO/CuPc/(CuPc+TPyP)/TPyP/Al with a mixed layer of CuPc and TPyP between them. In this paper we review the electrical and photovoltaic properties of some single-, two-, and three-layer organic photovoltaic cells, prepared and characterized in our laboratory. The photosensitization effect of a TPyP layer applied to a conventional a-Si:H based solar cell is also described.

2. Sample preparation and experimental procedures

Eastman Kodak Company supplied the CuPc dye and Aldrich-Chemie Company supplied TpyP. They were used without further purification. The chemical structures of dyes are illustrated the Figs. 1a), 1b).

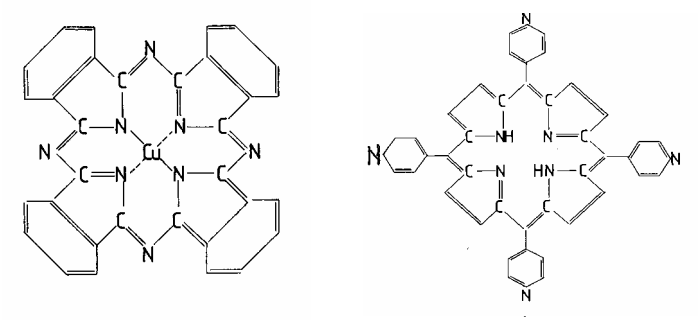

a b

Fig. 1. The chemical structural formula of: a) CuPc; b) TPyP

The many type of the investigated cells were prepared by the following procedure.

The indium tin oxide (ITO) coated glass provided the transparent conducting substrate (with transparency of 60% - 80%, for the average solar spectrum region), on which a layer of CuPc, TPyP, Chl-a on different thickness, were deposited by conventional vacuum evaporation. In the case of single-layer cells, a semitransparent top electrode was deposited on the organic layer, choused to form an ohmic or blocking contact at the interface organic/metal.

In the case of two-layer cells firstly was deposited on ITO, the organic layer having p-type conductivity, and over it the organic layer with n-type conductivity. Finally, a top electrode completed the structures. For the deposition of the mixed interlayer, in the case of three-layer cells, was carried out by the coevaporation of CuPc and TPyP from two separated sources, on the first deposited CuPc layer. The evaporation rates were separately controlled. We tried to obtain the volume ratio 1:1 for the mixed layers CuPc/TPyP. The total thickness of coevaporated layers was about 80 nm. A third layer of TPyP having the same thickness, was deposited on top of the codeposited layer, also by vacuum

evaporation. Finally, an Al layer was evaporated having an area of 0.25 cm^2 and defining the active area of the cell. The cells configurations, were generally shown as an inserts in figures showing their dark current-voltages characteristics. Both CuPc and TPyP are thermally very stable, thus allowing their deposition by vacuum evaporation. During sublimation the source temperature was maintained at about 380 °C for CuPc and at 280 °C for TPyP. The ITO transparent electrode has been found to form an ohmic contact with p-type CuPc and Chl-a and the Al electrode a nearly ohmic contact with the n-type porphyrin [5,10]. The current-voltage (I-U) characteristics in the dark were measured by biasing the devices with a voltage stabilised power source. The current and voltage were measured with a Philips microammeter and a Keithley 614 electrometer, respectively. The illumination of the cells was provided by a 650 W halogen lamp. A monochromator (spectral range of 300 to 800 nm) was used to obtain the spectral responses. The light power density at each wavelength has been measured with a powermeter to have the normalized spectra of photocurrent. The optical absorption spectra of the organic layers were obtained on a Perkin Elmer UV-VIS spectrophotometer (Lambda 2S). The power output of the cells was measured by introducing external resistance (10Ω-2TΩ) in the circuit.

3. Experimental results and discussion

3.1. The mono-layer cells based on CuPc and TPyP

3.1.1 ITO/CuPc/Al

The copper phthalocyanine (CuPc) is a p-type organic semiconductor having the hole equilibrium concentration $p_0 = 2.3x10^{13}$ cm^{-3}, the mobility $\mu_p = 1.1x10^{-2}$ cm^2/Vs, the dark electrical conductivity $\sigma_p = 4x10^{-8}$ $\Omega^{-1}cm^{-1}$ and the equilibrium Fermi level located at 0.455 eV above the valence band (VB), [13,23,27]. The prepared ITO/CuPc/Al cells [13], have asymmetrical I-U characteristics, Fig. 2, as a result of a contact barrier at Al/CuPc interface and an ohmic contact at ITO/CuPc interface. The photovoltaic response is due to the charge carrier fotogeneration in the organic layer and their separation in the built electric field present at Al/CuPc interface. The action spectra at illumination through the ITO electrode together with the absorption spectrum of the CuPc layer are shown in Fig. 3. The typical cell parameters at illumination through ITO electrode with monochromatic light (λ = 620 nm and ~10^5 photons/cm^2 s) are: the open-circuit photovoltage U_{OC} = 0.675 V, the short-circuit photocurrent I_{SC} = 8 nA, the fill factor ff = 0.35 and the power conversion efficiency $\eta_e = 0.6x10^{-2}$ %.

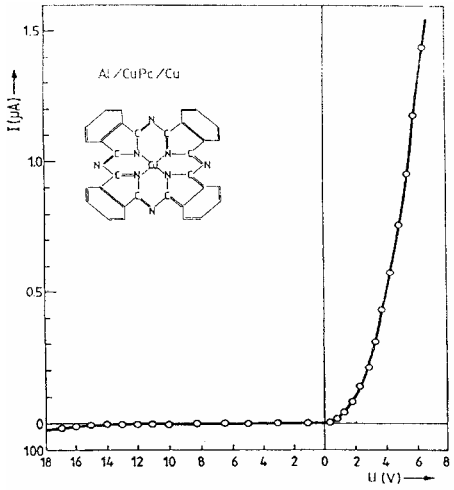

Fig. 2. The dark current - voltage characteristic of ITO / CuPc / Al cell at room temperature. The chemical structural formula of CuPc (inset).

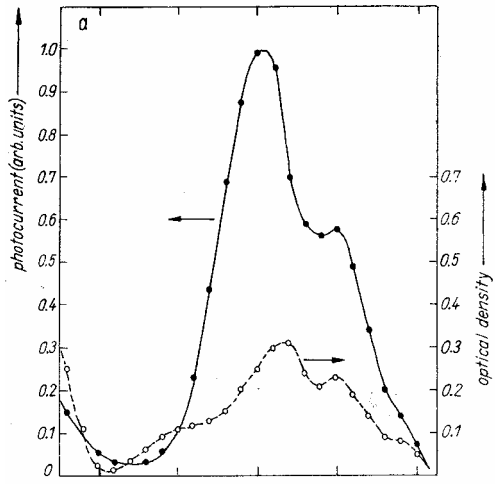

Fig. 3. Action spectrum of short - circuit photocurrent and absorption spectrum of the organic layers for the Schottky cells ITO/CuPc/Al.

3.1.2 ITO/TPyP/Al

The TPyP, differs from the majority of porphyrins and metal porphyrins in having n-type conductivity, due to the increase of electron affinity by the introduction of pyrydil groups in place of phenyl groups. From the analysis of the electrical and photovoltaic measurements made on the prepared ITO/TPyP/Al structures, it results that: a) the ITO/TPyP/Al sandwich cells show rectification and photovoltaic response, see Fig. 4, due to a Schottky barrier at the ITO/TPyP interface while Al/TPyP is Ohmic contact; b) the J-U characteristics at forward bias show Ohmic conductivity at low volatages and space-charge-limited conductivity at higher voltages; c) a thermally generated electron concentration of $n_0 = 3x10^9$ $cm^{-3}$was derived from the lower voltage-current density dependence and the equilibrium Fermi level is at $E_{F0} = 0.66$ eV below the edge of the conduction band.

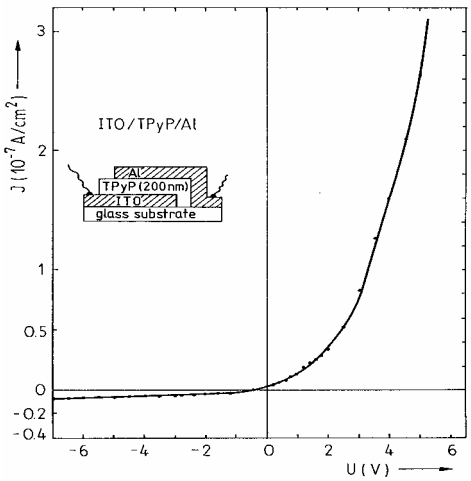

Fig. 4. The dark current – voltagc characteristic of ITO/TpyP/Al cell at room temperature.

Also from the ohmic region of J-U characteristics at different temperatures the values of the electron mobility $\mu_n = 6x10^{-4}$ cm^2/Vs and then the dark conductivity $\sigma_0 = 3x10^{-13}$ Ω^{-1} cm^{-1} were obtained.

From the space-charge-limited conductivity region, the following trap parameters resulted: $N_t = 1.7$ $x10^{14}$ cm^{-3}, E_c-$E_t = 0.75$ eV and $\theta = 5.5$ x 10^{-7}; d) the reverse J-U characteristics showed that Schottky effect is the dominant charge transport mechanism through the cells and derived parameters of the ITO/TPyP barrier were: $\Phi = 0.68$ eV and $w \in [193,50]$ nm when temperature increases from 295 to 360 K; e) the action spectra, Fig. 5, and the photovoltaic response, can be explained by considering that the photogenerated carriers are separated in the built-in field, extended over the whole thickness of the organic layer in agreement with the energy diagram shown in Fig. 6.

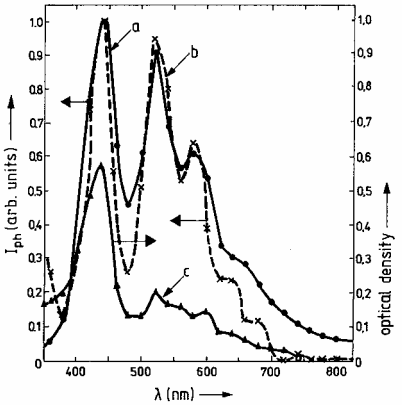

Fig. 5. Action spectrum and absorption spectrum of the ITO/TPyP/Al cell.

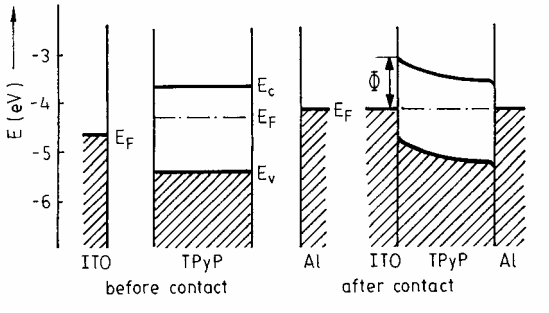

Fig. 6. Schematic representation of energy bands at the ITO/TPyP (50 nm)/Al junction. Φ is the barrier height at ITO/TPyP interface.

The typical cell parameters at illumination through ITO electrode with monochromatic light of 32 μ W/cm^2 at λ = 440 nm were: the open-circuit photovoltage U_{oc} = 0.175 V, the short-circuit photocurrent J_{sc} = 42 nA/cm^2, the fill factor ff = 0.13 and the power conversion efficiency η_e = 0.27x10^{-2}%.

3. 2. Two-layer organic photovoltaic cells

3.2.1 ITO/CuPc/TPyP/Al

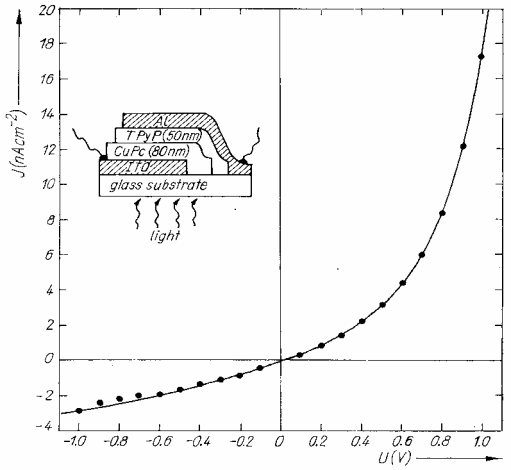

Fig. 7. Cell configuration (inset) and dark current-voltage characteristic of ITO/CuPc /TPyP/Al.

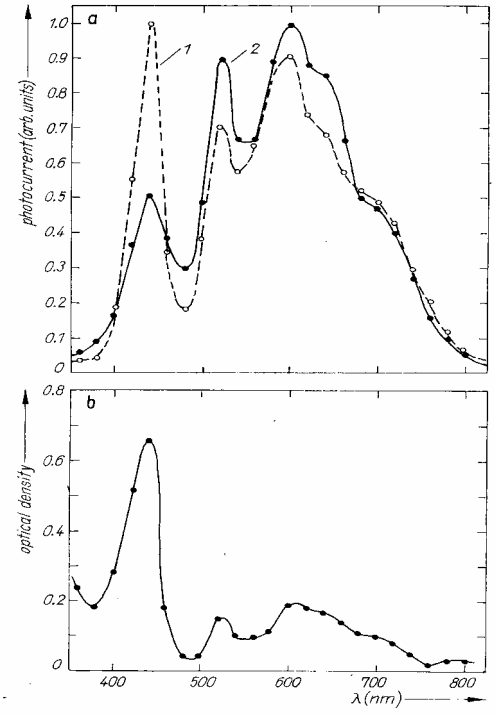

Fig. 8. a) Action spectra of short - circuit photo-current for the p-n junction cell of ITO/CuPc/ TPyP/Al. Curves (1) and (2) are obtained at illu-mination of the Al and ITO electrodes, respectively. (1) $J_{ph\ 400nm}$ = 0.845 nA/cm^2, (2) $J_{ph\ 600nm}$ = 223 nA/cm^2. b) Optical absorption spectrum of the CuPc/TPyP two layer film.

The combination of the two organic layers CuPc and TPyP in the ITO/CuPc(80 nm)/TPyP(50 nm)/Al p-n heterojunction cell, Fig. 7 led to an increase of power conversion efficiency by about two order of degree, with respect to ITO/CuPc/Al and ITO/TPyP/Al mono-layer cells, as a result of "cosensitization effect". Indeed the two organic layers with complementary absorption spectra are involved in the photogeneration processes.

The action spectra (Fig. 8), is larger than those of the single layer cells (Fig. 9). The resemblance of the two action spectra in Fig. 8, suggests that the region of maximum photosensitivity is at the CuPc/TPyP interface. A marked feature to be noted in Fig. 8a, is that curve 1 shows a distinct photocurrent maximum in the Soret band of TPyP film, while curve 2 has only a small peak around this band. In additions, in curve 2, the observed photocurrents in the range of broad absorption bands of CuPc film at wavelength from 500 to 750 nm, are greater than those in curve 1. Assuming that the photoactive region is the interface CuPc/TPyP, the above features in the action spectra, may be interpreted as follow: photons strongly absorbed in the Soret band of TPyP, are responsible for the maximum of photocurrent in curve 1, but also photons weakly absorbed in TpyP are participating in the photogeneration in the region of internal field from CuPc layer. Since the CuPc layer is thicker than the TPyP films, the maximum of photocurrent there is at the maximum of absorption in CuPc and the small photocurrent peak at the Soret band of TPyP, may be caused by attenuation of light reaching the p-n junction through the CuPc phase.

The J-U characteristic of the ITO/CuPc/TPyP /Al photovoltaic cell in the fourth quadrant of the J-U diagram is shown in Fig. 10. The cell was illuminated in monochromatic light of 20 $\mu W/cm^2$ at 440 nm and the charge resistors were varied in the range of 100 kΩ to 2 TΩ. The typical cell parameters have the following values: U_{oc} = 400 mV, J_{sc} = 135 nA/cm^2, ff = 0.44 and η_e = 0.12%. The value of the fill factor represents a substantial improvement as compared with the values of 0.12 and 0.13 obtained for single-layer cells ITO/CuPc/Al and ITO/TPyP/Al, respectively. The best power conversion efficiency, obtained under such illumination condition and without correction for the reflection or electrode absorption losses, was about 100 times greater than that for organic monolayer cells. Series resistance limits the conversion efficiency. It is large due to the thickness of the organic dye films.

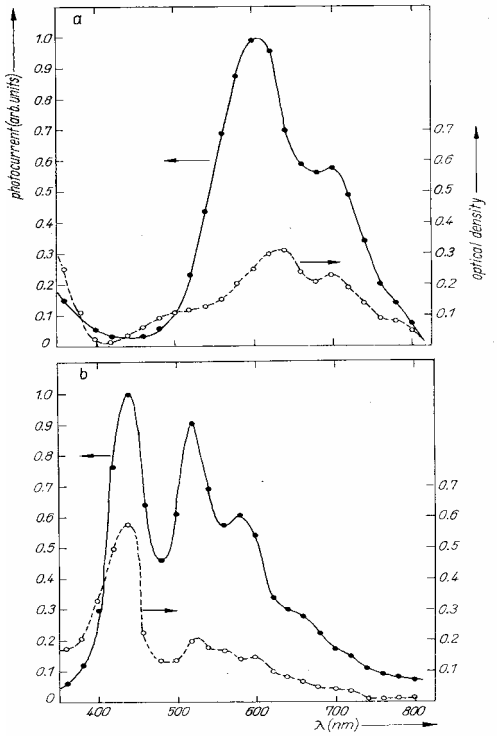

Fig. 9. Action spectrum of short - circuit photocurrent for the Schottky cells: (a) ITO/CuPc/Al; (b) ITO/TPyP/Al, at illumination through the ITO electrode, and the absorption spectrum of the: a) CuPc; b) TPyP layer. a) $J_{ph\ 600nm}$= 37.2 nA/cm^2, b) $J_{ph\ 400nm}$ = 28.8 nA/cm^2.

As concerning the model of operation, it was assumed that the absorption of light by both CuPc and TPyP layers creates excitons which can diffuse in the bulk of the films. At the interface or junction between the CuPc and TPyP layers the dissociation of excitons can take place, generating charge carriers. Therefore, holes are preferentially transported in the CuPc layer by the built-in field in p-n junction and are collected by the ITO electrode, while the electrons are transported in the TPyP layer towards the Al electrode. The observed polarity of the photovlotage, i.e. the CuPc layer is always positive with respect to the TPyP layer regardless of the electrode materials, is strongly indicative of conduction type in the two layers.

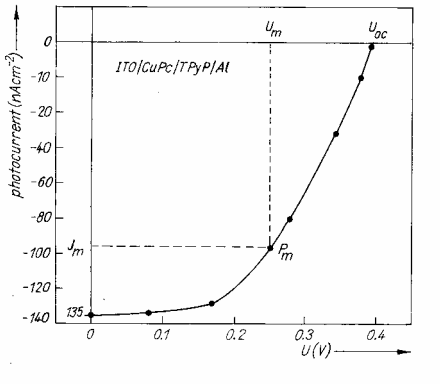

Fig. 10. Current - voltage characteristic for ITO/CuPc/TPyP/Al photovoltaic cell in the fourth quadrant, under illumination with monochromatic light of 20 μW/cm^2 at 440 nm.

3.2.2 ITO/Chlorophyll a /TPyP/Al

Fig. 11 shows the dark-current density through a typical ITO/Chla(200 nm)/TPyP(100 nm)/Al cell as function of applied bias at room temperature. Chla is considered to be a p-type semiconductor, with high work function of ~ 4.5 eV and the ITO electrode, having work function of about ~4.7 eV forms an ohmic contact, at the interface ITO/Chla. TPyP being a n-type semiconductor, with a low work function of ~4.1 eV [14], forms an ohmic contact with Al. Since Chla and TPyP make ohmic contacts with ITO and Al electrodes respectively, we infer that the rectification shown in the bipolar J-U characteristic in Fig. 11, is due to the energy barrier at the Chla/TPyP interface.
Fig. 12b shows the action spectrum of the p-n heterojunction ITO/Chla(200nm)/TPyP(100nm)/Al cell (1), together with the action spectra of the Schottky type cells: ITO/Chla(200nm)/Al (2) and ITO/TPyP(100nm)/Al (3), respectively. All the spectra are obtained by illumination on the ITO electrode. Fig. 12a shows the optical absorption spectrum of Chla/TPyP (a), Chla (b) and TPyP (c) films, respectively, used in the fabrication of sandwich cells. For all action spectra in Fig. 12b the photocurrents are divided by the number of photons incident on the ITO electrode for each wavelength and then normalized to unity.

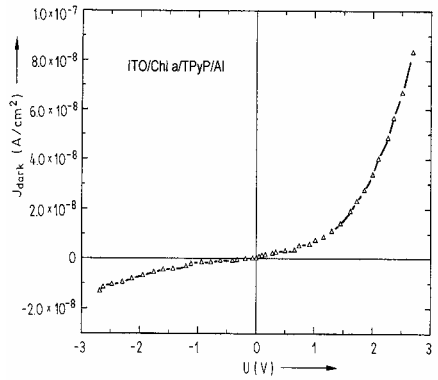

Fig. 11. Current - voltage characteristic of ITO/Chl a(200 nm)/TPyP (100nm) cell in the dark at room temperature.

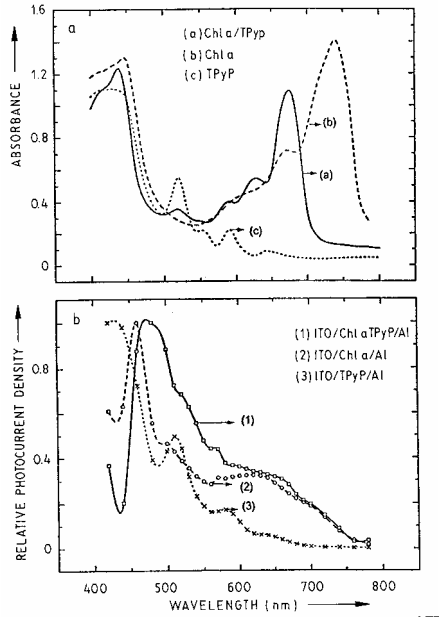

Fig. 12.a) Absorption spectrum of Chl a/TPyP films (a), Chl a layer (b), and TPyP layer (c). b) Action spectra of cells illuminated through ITO: ITO/Chl a/Al (1), ITO/Chl a/Al (2), and ITO/TPyP/Al (3).

The action spectrum of the two-layer cell, when illuminated through ITO electrodes matches better the absorption spectrum of TPyP film than of Chla film. This behavior suggests that the singlet excitons are the precursors of the charge carriers and that the space-charge region is at the Chla/TPyP interface. In other words, only those excitons created in the barrier region or having diffused into it contribute to the photocurrent. The photocurrent generation in the p-n heterojunction cell, as compared with that in the Schottky cells, Fig. 12.b, curves (2) and (3), is strongly enhanced at the wavelengths corresponding to the absorption peaks of the organic and biologic layer. The photocurrent measured at 460 nm is about three times greater in the case of ITO/Chla/TPyP/Al cell than that of ITO/Chla/Al cell, while the photocurrent of p-n heterojunction cell measured at 670 nm is about seven times greater than that of ITO/TPyP/Al cell. The appearance of a large photocurrent at wavelengths corresponding to the Soret region of Chla absorption spectrum can be explained by the photogeneration of charges in TPyP layer in addition to the charge generation in Chla layer. The larger photocurrent of p-n heterojunction cell at 670 nm is due to the charge photogenerated mostly in Chla layer. All the compared action spectra were obtained at illumination through the ITO electrode. The ratio of area covered by the action spectra of ITO/Chla/TPyP/Al , ITO/Chla/Al and ITO/TPyP/Al cells is 144:123:87 – Fig. 12.b, pleading for a " cosensitization effect" in the case of ITO/Chla/TPyP/Al two-layer cell.

The fourth quadrant of J-U characteristic of ITO/Chla/TPyP/Al photovoltaic cell is presented in Fig. 13. The cell was illuminated by monochromatic light of 20 $\mu W/cm^2$ at 470 nm and the charge resistors were varied in the range 100 kΩ to 2 TΩ . The typical photovoltaic cell parameters, open circuit photovoltage (U_{oc}), short photocurrent density (J_{sc}) and fill factor (ff) under the mentioned illumination conditions, have the following values: U_{oc} = 490 mV, J_{sc} = 13 $nAcm^{-2}$ and ff = 0.34. The fill factor of 0.34 represents a substantial improvement as compared with the values of 0.09 and 0.13 obtained for ITO/Chla/Al and ITO/TPyP/Al Schottky cells, respectively. The power conversion efficiency, obtained under the mentioned conditions of illumination and without correcting for reflection or electrode absorption losses, was ~ 1.1×10^{-2}%, about 2-3 times higher than the value obtained for ITO/Chla/Al cell. The conversion efficiency is strongly limited by the high internal resistance, ~200MΩ, due to the thickness of Chla and TPyP films.

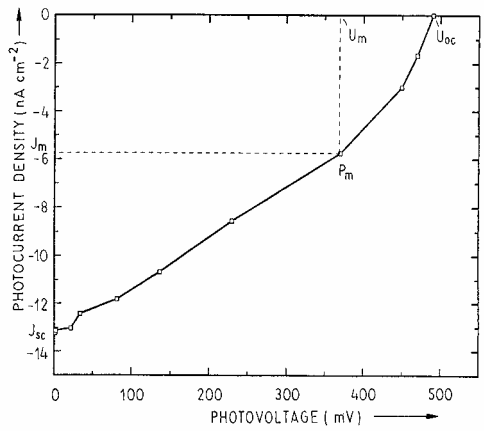

Fig. 13. Current - voltage characteristic for the ITO/Chl a/TPyP/Al cell in the fourth quadrant, under illumination with monochromatic light of 20 μW/cm^2 at 470 nm.

3. 3. Three - layered photovoltaic cell with an enlarged photoactive region of co-deposited dyes

3.3.1. ITO/CuPC/(CuPc+TPyP)/TPyP/Al

Dark current-voltage characteristics

Fig. 14 shows the dark current through a typical ITO/CuPc/(CuPc+TPyP)/ TPyP /Al cell as a function of the applied bias, at room temperature.

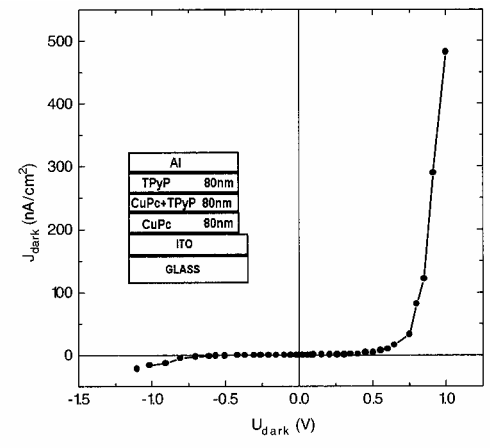

Fig. 14. Cell configuration (insert) and the dark current-voltage characteristic of the ITO/CuPc /(CuPc+TPyP)/TPyP/Al cell at room temperature.

The forward bias corresponds to a positive voltage on ITO with respect to Al electrode. The cell exhibits a strong rectifying effect in the dark, characterized by the rectification ratio (forward bias current/reverse bias current) of nearly 500 at the voltage of 1 V. For a rigorous analysis of (I-U) curves with respect to conduction mechanisms and cell parameters, firstly we found out the implication of Shockley mechanism by seeking out the linear region in the ln(I)-U plot of the forward current-voltage characteristics of the cell. The forward characteristic of the cell up to 1V can be fitted well by the modified Shockley equation:

$$I = I_0\left\{\exp\left[\frac{q\left(U - IR_s\right)}{nkT}\right] - 1\right\} + \frac{U - IR_s}{R_{sh}} \tag{1}$$

where: I_0, n, R_s and R_{sh} are the reverse saturation current, diode quality factor, series and shunt resistance of the cell, respectively and q is the electronic charge.
From Eq.(1), the junction resistance , R_0, is:

$$R_0 = dU/dI = R_s + 1/\left\{\beta I_0 \exp\left[\beta\left(U - IR_s\right)\right] + 1/R_{sh}\right\} \tag{2}$$

where β=q/nkT.
For higher forward bias, where R_s affects the curves, Eq. (1) can be approximated as $I = I_0\exp[\beta(U-IR_s)]$, and since $1/R_{sh} < \beta I$, Eq.(2) can be written as follows:

$$R_0 \cong R_s + 1/\beta I \tag{3}$$

Thus by plotting R_0 vs $1/\beta I$ for high forward biases, one can obtain R_s and the value of n. For low voltages, where R_{sh} acts, the approximation $\beta I_0\exp[\beta(U-IR_s)] << 1/R_{sh}$ is valid, and Eq.(2) becomes:

$$R_0 \cong R_s + R_{sh} \tag{4}$$

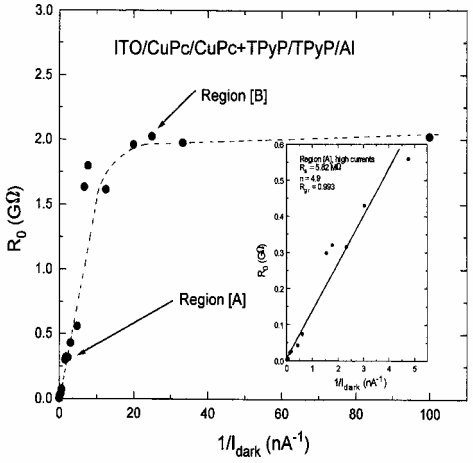

Fig. 15. The variation of junction resistance R_0 as a function of reciprocal forward current 1/I. The insert zooms on region A of high currents.

Usually $R_s << R_{sh}$, R_0 thus approaches R_{sh} at low biases. The graph of R_0, the junction resistance, versus 1/I is shown in Fig.15, for one of our three-layered cell. One can divide the plot in two regions: A and B, for high and low forward currents respectively. For region [A] (expanded in the insert), one notices that R_0 as a function of 1/I shows linearity up to the applied voltage of ~ 0.7 V (the voltage from J-U plot in Fig. 15, corresponding to the value 0.6 GΩ of R_0) and curves thereafter, for high forward biases. From the extrapolated linear region A, the determined value of R_s is 5.82 MΩ; the value of R_{sh} , obtained from region [B] being ~ 2 GΩ.

To improve the linearity of ln(I)-U plot, for determination of n and I_0, we first remove the effect of R_s. This is achieved by making the following change in variable:

$$Y = U - IR_s \tag{5}$$

With this change, Eq. (1) becomes:

$$I = I_0[\exp(\beta Y) - 1] + Y/R_{sh} \tag{6}$$

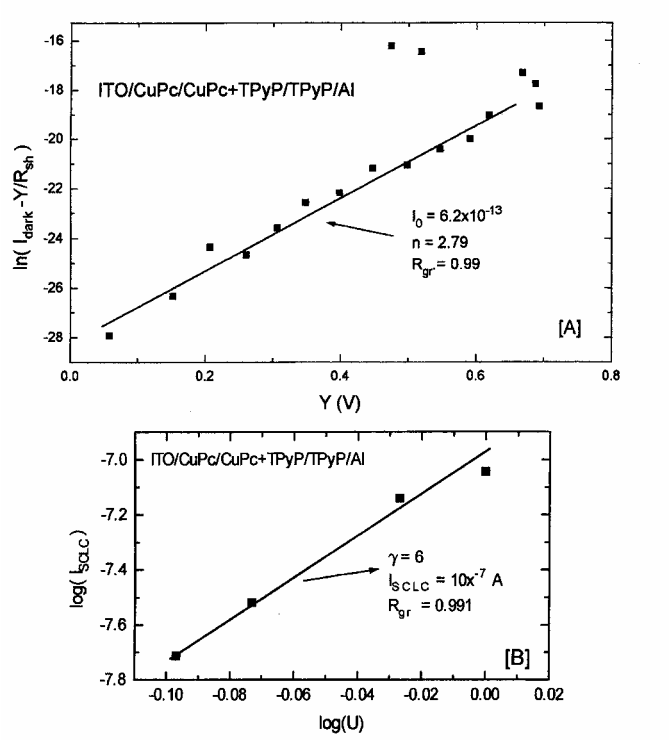

Fig. 16. [A] Semilogarithmic plots of the forward-biased dark current: I-Y/R_{sh} vs Y. [B] Logarithmic plot of SCLC current vs voltage for high forward biases.

where Y is the voltage only across the junction. For high forward biases, Eq.(6) can be written as:

$$I \cong I_0 \exp(\beta Y) \tag{7}$$

Thus, from the plot of lnI vs. Y, n and I_0 can be determined. Further, to increase the precision it is advisable to remove the effect of R_{sh} from the ln(I)-U plot, as well. This is achieved by plotting ln(I-Y/R_{sh}) vs. Y, because (I-Y/R_{sh}) can be considered to describe the current flowing in the diode junction only. Such a plot for our cell is shown in Fig. 16[A]. One can see that the removal of R_{sh} and R_s has lead to the increase in the linearity of the curve at lower biases from 0.3V to 0.1V and at higher biases from 0.7 to 0.8 V, respectively. Then the whole linear region of ln(I)-U plot is extended in the range 0.1-0.8V. The values of n and I_0 obtained from the slope and the intercept are 2.79 and $6.2x10^{-13}$A, respectively and are more reliable than those obtained after the removal of R_S only. For biases > 0.8V, the current shows a power dependence of voltage, i.e. follows the relation $I \sim U^m$ where m = 7, as seen from log(I)-log(U) plot in Fig.16[B]. This superquadratic power dependence suggests that the dark current is a space-charge-limited-current (SCLC) in the presence of exponentially distributed traps. According to Mark and Helfrich [15], the SCLC for a solid with a trap distribution decreasing exponentially with the trap depth is given by:

$$J_{SCLC} = N_{eff}\,\mu q^{1-\gamma}\,[\varepsilon\gamma/N_t(\gamma+1)]^{\gamma}\,[(2\gamma+1)/(\gamma+1)]^{\gamma+1}\,(U^{\gamma+1}/d^{2\gamma+1}) \tag{8}$$

where N_{eff} is the effective density of states in conduction or valence band, and $\gamma = T_c/T$, T_c is a "characteristic temperature", that describes the trap distribution.

The Photovoltaic Properties

The photovoltaic action spectra can provide considerable information as regarding to how the charge carriers are generated. The action spectra of short-circuit photocurrents of ITO/CuPc/(CuPc+TPyP)/TPyP/Al [A] and ITO/CuPc/TPyP/Al [B] cells are shown in Fig.17, while the absorption spectra of the organic layers CuPc and TPyP are shown in Fig. 18. The action spectra

are measured at illumination through the ITO electrode. These are obtained by plotting the short-circuit photocurrent J_{ph} divided by the number of incident photons on the ITO/CuPc interface and then normalised to unity. Although the absorption spectra of TPyP and CuPc layers, are nearly complementary (the main maxims of TPyP and CuPc layers are centred at 430 and 620 nm, respectively), both the TPyP and CuPc layers contribute to the photogeneration of carriers in the two cells. A marked feature to be noted in Fig. 17 is that both curves show greater photocurrents in the range of the broad absorption band of CuPc film (at wavelength between 500 and 750 nm). In the Soret region of all action spectra presented in Fig. 17, a distinct peak appears, as a result of the photons weakly absorbed in CuPc, but strongly absorbed in the Soret band of TPyP.

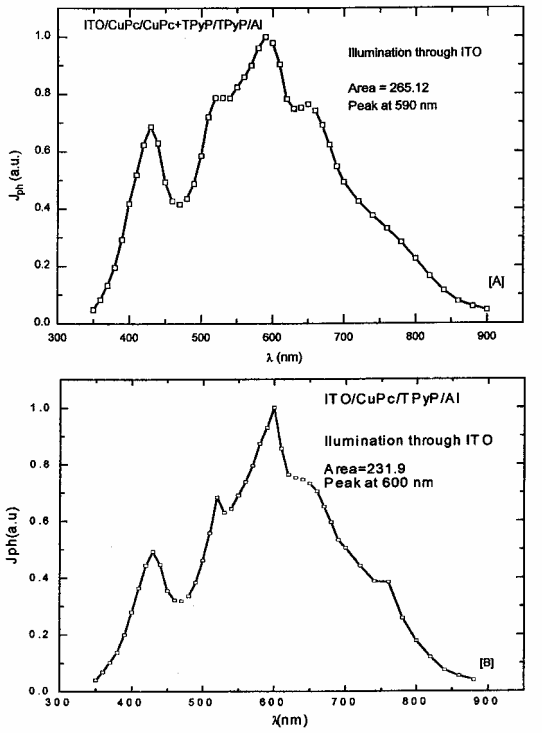

Fig. 17. The action spectra of the cells:
[A] ITO/CuPc/(CuPc+TPyP)/TPyP/Al ;
[B] ITO/CuPc/TPyP/Al , illuminated through ITO electrode.

It is important to note that, although moderate absorption there is both in TPyP and CuPc layers at wavelength of 520nm, Fig. 18, a peak of photocurrent exists at this wavelength, which is greater than that from Soret band of TPyP. The filtering effect of CuPc layer has to be considered. This behaviour shows strongly that the photoactive region (i.e. in the internal field region) there is at the CuPc/TPyP interface.

The photocurrent of the three-layered cell Fig. 17 [A], was about ten times larger than that of two-layered cell Fig. 17.[B] all over the spectral region. The thickness of the front CuPc layers is the same (80nm) in both typed cells, i.e. the same masking effect due to CuPc layer. This result strongly suggests that the codeposited interlayer, which has a large amount of direct molecular contacts between TPyP and CuPc molecules and consequently there is a thicker depletion region, may provide an efficient carrier photogeneration layer. It is known [2] that an efficient photogeneration mechanism is that of exciton dissociation on the doping complex states present in the volume of an organic photoconductor. That is why, presently, we suspect that the charge photogeneration via exciplex of the two dyes, i.e. $(TPyP^{-} ....CuPc^{+})^{*}$, from codeposited layer is responsible for the efficient photogeneration of the charge carriers. The better agreement of the absorption spectrum of the codeposited layers and the action spectra of the cells illuminated through ITO electrode, suggests that

the singlet excitons are the precursors of the charge carrier by the previous described process and that the photovoltaic region is located in the codeposited interlayer.

The dependence of the short-circuit photocurrent (J_{sc}) on the incident light intensity (I_{inc}), when illuminated through ITO, was examined too. At the wavelengths 520 and 590 nm, the dependence of (J_{sc}) vs (I_{inc}) of the cell follows the relation $J_{sc} \sim I_{inc}^{m}$, where the exponent m < 1. This is a common behaviour for the organic photovoltaic cells and could be explained by taking into account the model based on the combined effect of traps and recombination centres [3,4,5,7].

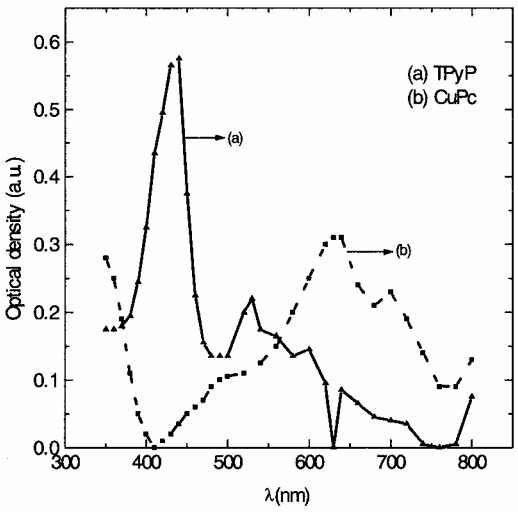

Fig. 18. The absorption spectra of (a) TPyP and b) CuPc layers.

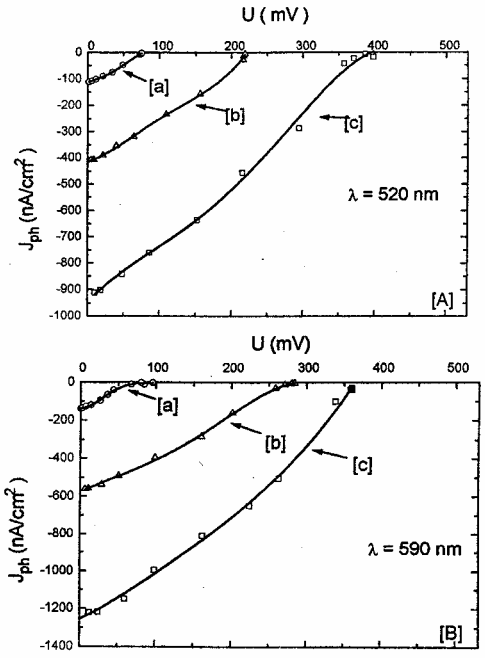

Fig. 19. Photocurrent- photovoltage characteristics of the ITO/CuPc/(CuPc+TPyP)/TPyP/Al cell illuminated through ITO electrode with:
[A] 520 nm wavelength of varying intensity as (3 μW/cm^2 [a], 12 μW/cm^2 [b] and 30 μW/ cm^2 [c]); [B] 590 nm wavelength of varying intensity as (6 μW/ cm^2 [a], 30 μW/ cm^2 [b] and 72 μW/ cm^2 [c]).

Fig. 19 [A],[B] show the (J_{ph} -U) characteristics in the fourth quadrant of (J-U) diagram of a typical ITO/CuPc/(CuPc+TPyP)/TPyP/Al cell, obtained at 520 and 590 nm, the wavelengths where a high sensitivity of the cell exists. These curves were obtained by varying the load resistance in the range 100 kΩ to 2 TΩ at constant input light intensities, which are given in the legend of each plot. Several parameters of interest such us open-circuit photovol-tage (U_{oc}), short-circuit photocurrent (J_{sc}), fill factor (ff) and power conversion efficiency (η) can be evaluated from these curves and are listed in Table 2.

a) The fill factor defined as ratio of the maximum output power density to the product (U_{oc}*J_{sc}) gives a measure of how close the cell is to an ideal photovoltaic cell (ff = 1). The fill factors of this particular cell have different values ranging from 0.11 to 0.32. The low fill factors obtained for this cell are comparable to other organic photovoltaic cells [3,5,6,10], but generally larger than of single and two-layered organic cells. This low values are due to two separate effects, namely, the high series resistances and the field-dependent nature of the photogeneration of charge carriers [2,8]. The highest value of fill factor was obtained at 520 nm for 3 μW/cm^2, and smaller values were obtained for higher light intensities at all wavelengths.

b) The power conversion efficiency has been evaluated from the following relation

$$\eta(\%) = \frac{ff \times J_{sc} \times U_{oc}}{I'_{inc}} \times 100 \qquad (9)$$

where I'_{inc} is the light power density incident on the cell corrected for the transparency of ITO electrode. The efficiencies calculated at 520 and 590 nm, for various values of the input power are listed in Table 2.

Table 2. The typical parameters of ITO/CuPc/(CuPc+TPyP)/TPyP/Al cells.

λ (nm)	Curve See Fig.	I'_{inc} (μ W/cm^2)	J_{sc} (nA/cm^2)	U_{oc} (mV)	ff	η (%)
520	[a]	3	107	75	0.32	0.09
520	[b]	12	410	220	0.29	0.22
520	[c]	30	916	405	0.28	0.35
590	[a]	6	136	87	0.23	0.05
590	[b]	30	528	277	0.31	0.15
590	[c]	72	1250	350	0.11	0.07

The better performance of the cell are obtained for more penetrating 520 nm wavelength where the values 0.09, 0.22 and 0.35% for 3, 12 and 30 μW/cm^2 input powers have been resulted. These values of η are about 2-3 times larger than those of a two-layer cell and are among the best reported for organic solar cells. The better performance of the cell at shorter wavelength is most probable due to the bulk ionisation of more energetic 520 nm excitons into charge carriers, mainly in TPyP layer. One can observe that for this wavelength the efficiency increases when the light intensity increases. At longer wavelength, such as 590 nm, the efficiency increases when the intensity increases up to 30μW/cm^2 and decreases when the light intensity increases further. This decrease is mostly due to the above evaluated dependence of J_{sc} on I_{inc} and can be understood in terms of a physical model involving traps and recombination centres [16]. As the light intensity is increased, the electron and hole densities increase and therefore the quasi-Fermi levels are moving toward the conduction and valence bands, respectively. As the light intensity is further increased, more and more of the trapping states are converted into recombination centres, thus reducing the lifetime of charge carriers and resulting into non-linear variation of photocurrent with light intensity. As regarding the open-circuit photovoltage, both double- and three-layered cells showed almost the same magnitude for U_{oc}, about 0.4 V as an average value. This result tells us that the built-in potential for both typed cells originates from the difference of Fermi levels between CuPc and TPyP layers. We suppose that most of built-in potential is distributed across the interlayer. Since positive charges of ionic donors in n-type TPyP and negative charges of ionic acceptors, in p-type CuPc are com-pentad with each other, the codeposited layer behaves like an intrinsic semiconductor and then the three-layered cell resembles with a p-i-n a-Si:H based solar cell.

As a conclusion, this new type of three-layered organic photovoltaic cells having a codeposited layer of (CuPc +TPyP), between the CuPc and TPyP films, clearly suggest an improvement, although modest, over two-layered cells. The codeposited interlayer, has been found to act as an efficient carrier photogeneration layer because: on one hand, the built-in potential drops across it and on the other hand, here there is the region of maximum photogeneration rate, as a result of exciton dissociation via the exciplex of $(CuPc^{-}$ ....$TpyP^{+})^{*}$ dyes. The fill factors of 0.11-0.32 represent an improvement over single and double-layered cells. Moreover, the power conversion efficiencies of three-layered cells, ranging from 0.07 to 0.35%, are 2-3 times greater as compared to those for double-layered cells. The thickness of about 0.4μm of our three-layered cells is mainly responsible for the high internal resistance, which limits again the performances of the cells. By obtaining of an optimised structure as regarding the thickness of the layers and the architecture of the cells, we are convinced that substantial improvement of the organic photovoltaic cells would be possible.

3.4. Electrical and photovoltaic properties of photosensitized ITO/a-Si:H p-i-n/TPyP/Au cells

The dark current-voltage (I_d-U) characteristics of the ITO/a-Si:H p-i-n/TPyP/Au is shown in Fig. 20, containing as inset the crossection of the cell. The characteristic is asymmetric having very high rectification ratio ($R_r = 10^4$ at 0.6 V). The behavior of the mentioned structure is due to the energy barrier at the p-i interface, both ITO and Au electrodes giving ohmic contacts with the semiconductor layers. To the interface a-Si:H/TPyP, there is no energy barrier (a-Si:H and TPyP have about the same work functions). The parameters n and I_0, having the values: 2.6 and $1.14x10^{-10}$ A, respectively, have been deduced by the same procedure, used in the case of previous structures. Summarizing, the analysis of the dark current-voltage characteristics has suggested that the ITO/a-Si:H p-i-/TPyP/Au cell can be considered as p-i-n junction combined with R_s (which is mainly due to the organic layer) .

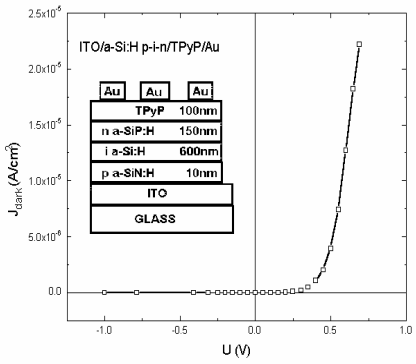

Fig. 20. Cell configuration (inset) and current-voltage characteristics of ITO/a-Si:H p-i-n/TPyP/Au cell.

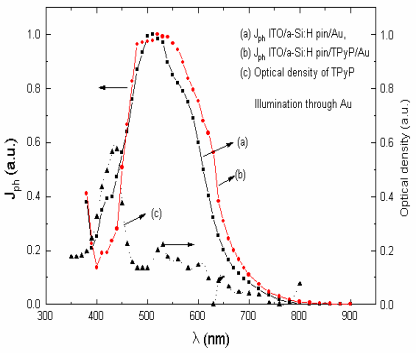

Fig. 21. The action spectra of short-circuit photocurrent of: (a) ITO/a-Si:H p-i-n/Au and (b) ITO / a- Si:H p-i-n /TpyP /Au cells. (c) Optical absorption spectrum of TPyP layer.

Fig. 21 shows the action spectra of the short-circuit photocurrent for both ITO/a-Si:H p-i-n/Au (a) and ITO/a-Si:H p-i-n/TPyP/Au (b) structures respectively, as well as the absorption spectrum (c) of the TPyP layer. A marked feature to be noted in Fig. 21 curve (b), is that the presence of the TPyP film give rise to a shift of the long-wavelength edge of the action spectrum of approximately 30 nm to longer wavelengths. The maximum of photocurrent from 500 nm of nonsensitised cell is shifted to 530 nm in the case of the sensitized cell. Looking the absorption spectrum of the TPyP layer Fig. 21, (c), we can see that the main absorption peaks from 430 nm, 520 nm, 620 nm, are reflected in the action spectrum of the sensitized cell (curve (b)). The area of curve (b) is also larger than that of curve

(a). These observations suggest that the sensitization involves an increase of the number of the charge carriers within the a-Si: H p-i-n cell, due to organic layer.

Because TPyP is a n-type semiconductor, the charge displacement within the cell arises from supplemental injection of electrons from the sensitizing layer. The general mechanism of spectral sensitization is: the absorption of the photons in the TPyP creates excitons which diffuse to TPyP/a-Si: H interface, where they dissociate to create free electron-hole pairs. The electrons are injected into TPyP and the holes are displaced by the internal electric field to p-type layer of a-Si: H.

4. Conclusions

1. The single - layer ITO/CuPc/Al and ITO/TPyP/Al cells have a photovoltaic response as a result of the charge carrier photogeneration in CuPc or TPyP layer and their separation in the built electric field present at Al/CuPc and ITO/TPyP interface, respectively. The values of the typical cell parameters (U_{oc}, I_{sc}, ff, and η_e) are in good agreement with those of other organic monolayer cells.
2. The two-layer ITO/CuPc/TPyP/Al cells have a power conversion efficiency of about 100 times greater than that of organic monolayer cells, due to a strong cosensitization effect. The ITO/Chla/TPyP/Al cells show rectification and photovoltaic phenomena due to barrier formed at the Chla/TPyP interface. Various photovoltaic features of ITO/Chla/TPyP/Al cells suggest an improvement, although modest, over ITO/Chla/Al cells.
3. The three-layered organic photovoltaic cells (ITO/CuPc/(CuPc +TPyP)/TPyP/Al), clearly suggest an improvement, although modest, over two-layered cells. The codeposited interlayer, has been found to act as an efficient carrier photogeneration layer because: on one hand, the built-in potential drops across it and on the other hand, here there is the region of maximum photogeneration rate, as a result of exciton dissociation via the exciplex of $(CuPc^- ....TpyP^+)^*$ dyes. The fill factors of 0.11-0.32 represent an improvement over single and double-layered cells. Moreover, the power conversion efficiencies of three-layered cells, ranging from 0.07 to 0.35%, are 2-3 times greater as compared to those for double-layered cells.
4. The spectral sensitization of an a-Si: H solar cell using an organic layer was obtained. The action spectrum was extended by 30 nm to longer wavelengths range, using a 100 nm thick layer of TPyP. The sensitization is explained by an exciton dissociation process to the TPyP/a-Si: H interface, which gives rise of higher quantum efficiency at longer wavelengths.

References

[1] K. Ghosh, T. Feng, J. Appl. Phys. **49**, 5982 (1978).
[2] G. A. Chamberlain, Solar Cells, **8**, 47 (1983).
[3] Fu-Ren Fan, R. Faulkner, J. Chem. Phys., **69**, 3334 (1978).
[4] K.Yamashita, Y. Matsumura, Y. Harima, S. Miura, H. Suzuki, Chem. Letters, **4**, 489 (1984).
[5] S. Antohe, L. Tugulea, Phys. Stat. Sol. (a) 128, 253 (1991).
[6] S. Antohe, Rev. Roum. Phys., **37**(3), 309 (1992).
[7] F. J. Kampas, M. Gouterman, J. Phys. Chem., **81**, 690 (1977).
[8] W. A Nevin, G. A. Chamberlain, J. Appl. Phys., **69**, 4324 (1991).
[9] S. Antohe, Phys. Stat. Sol. (a), 136, 401 (1993).
[10] Y. Harima, K. Yamashita, H. Suzuki, Appl. Phys. Lett., **45**, 1144 (1984).
[11] C. W. Tang, Appl. Phys. Lett., **48**(2), 183 (1986).
[12] M. Hiramoto, H. Fujiwara, M. Yokoyama, Appl. Phys. Lett., **58**(10), 1062 (1991).
[13] S. Antohe, I. Munteanu, I. Dima, Rev. Roum. Phys., **34**(6), 665 (1989).
[14] A. Oueriagli, H. Kassi, S. Hotchandani, R. M. Leblanc, J. Appl. Phys., **77**(11), 5523 (1992).
[15] P. Mark, W. Helfrich, J. Appl. Phys., **33**, 205 (1962).
[16] H. Meier, Organic Semiconductors, Verlag Chemie, Weinheim, (1974).
[17] A.K. Ghosh, D.L. Morel, R.F. Show, C.A. Rowe Jr., J.Appl.Phys., **45**, 230, (1974)

[18] C. W. Tang, A. C. Albrecht, J. Chem. Phys., **63**, 953, (1975)
[19] F. R. Fau, L. R. Faulkner, J. Chem. Phys., **67**, 3341, (1978)
[20] G. A. Chamberlain, R. E. Malpas, Faraday.Discuss.Chem.Soc., **70**, 229, (1980)
[21] G. A. Chamberlain, P. J. Cooney, S. Denison, Nature, **289**, 45, (1981)
[22] A. M. Hor, R. Loutfy, Thin Solids Films, **106**, 291, (1983)
[23] S. Antohe, I. Munteanu, I. Dima, N. Tomozeiu, V. Mitache, Lucrarile CAS'89, Ed. a-12-a, Sinaia, RO, 1989, p.65
[24] S. Antohe, L. Tugulea, V. Gheorghe, V. Ruxandra, I. Cåplånus, L. Ion, Phys. Stat. Sol. (a) 153, 581 (1996)
[25] S. Antohe, V. Ruxandra. L. Tugulea, V. Gheorghe, D. Ionascu, J. Phys. III France 6, 1133 (1996).
[26] L. Tugulea, S. Antohe, Research in Photosynthesis, II, 845, (1993)
[27] S. Antohe, I. Dima, I. Munteanu, Lucrarile CAS'87, Ed. a-10-a, Sinaia, RO, 1987, p.63
[28] S. Antohe, L. Ion, N. Tomozeiu, T. Stoica, E. Barna, Solar Energy Materials & Solar Cells 62, 207 (2000).